Proceedings of the Twenty-third (2013) International Offshore and Polar Engineering **www.isope.org**
Anchorage, Alaska, USA, June 30–July 5, 2013

ISBN 978-1-880653-99–9 (Set); ISSN 1098-6189 (Set)

Effect of Short-crested Waves on the Dynamic Responses of Truss SPAR Platforms

V.J. Kurian, C.Y. Ng and M.S. Liew
Civil Engineering Department, Universiti Teknologi PETRONAS
Bandar Seri Iskandar, Tronoh, Perak Darul Ridzuan, Malaysia

ABSTRACT

Short-crested wave in real sea condition is defined as the linear summation of a series of long-crested waves propagated to different directions, where the magnitude and directions are randomly generated. Also, it is complex and three dimensional. In this paper, an experimental and numerical study on the truss spar responses subjected to long and short-crested waves are presented. The experimental study on a typical truss spar model subjected to long and short-crested waves were performed in the wave tank of Offshore Laboratory in Universiti Teknologi PETRONAS. In the study, physical motions in surge, heave and pitch of the model with four linear spring mooring lines restrained were measured. Also, a numerical MATLAB code incorporating the short-crestedness of the waves to predict the dynamic analysis of the truss spar was developed. The results were obtained in terms of Response Amplitude Operator (RAO) for surge, heave and pitch motions using both methods. The predicted RAO were compared with the measured RAO and they agreed fairly well. Also, it was observed that the responses for short-crested waves were much lower compared to the responses for long-crested waves.

KEY WORDS: Short-crested waves; model test; truss spar; dynamic responses; response amplitude operator.

INTRODUCTION

Wind, wave, and current are the dominant environmental forces acting on offshore structures. Among these, wave force contributes almost 70% of the total lateral force. Based upon the direction of the wave propagated, it has been categorized as long or short-crested. Waves that head in one direction are called long-crested waves, while the waves heading to two or more directions are called short-crested waves. The wind-generated seastate in the real sea condition is more appropriate to be considered as short-crested waves (Jian et al, 2008). Also, short-crested waves can be considered as complex and three dimensional (Chakrabarti, 2001).

Studies focusing on directional wave force, directional wave spectrum, directional wave kinematics, and vertical circular cylinder on short crested waves have been done since 1970s. Zhu (1993) presented a solution for bottom-seated vertical circular cylinder subjected to diffraction of incident short-crested waves. Then, Zhu and Moule (1994) presented the study on short-crested wave forces exerted on vertical cylinder with circular, elliptical and square cross sections. A closed-form solution up to second order wave amplitude for the velocity potential of nonlinear short crested waves was presented by Zhu and Satravaha (1995). This theory was extended by Jian et al (2008) to incorporate the effect of uniform current for different incident angles. In their study, the analytical solution was derived for short-crested diffraction along positive x-axis direction on a large circular cylinder.

Directional waves were not widely used for design purposes due to limited resources of measured directional data for waves. Hence, Borgman (1969) introduced a directional spectral model for the design of offshore structures. Fernandes (2000) studied the directional wave spectrum measured by the phase-time-path-difference method. Directional wave spectrum measured and estimated by the high frequency ocean radar was performed by Hisaki (2006). A solution for modeling a parametric directional spectrum that takes account of the wind-generated sea and swell wave was introduced by Hogben and Cobb (1986). Aage (1990) proved that the 3D wave load exerted on a cylinder is smaller than 2D wave load with identical spectra or even identical wave elevation time series, in his study about the safety using the reduced 3D loads in offshore design.

Directional wave spectra are defined as a product of frequency or point spectrum and spreading function. The common spreading function considered as such as cosine square, cosine^6, stereo wave observation project (SWOP) and Mitsuyasu etc. Kumar et al (2000) studied the characteristics of directional spreading parameters at the intermediate water depth by cosine 2s directional spreading model. Also, they studied the effects of wave directional spreading in shallow water and variations in estimating the wave direction using the first and second order Fourier coefficients (Kumar et al, 1999; Kumar et al, 2004).

In this paper, an experimental wave tank test, focusing on the dynamic motion responses of a truss spar model subjected to long and short-

crested wave was performed to evaluate the effectiveness of the short-crested wave statistics for the design of offshore structures. The dynamic motion responses of the model were estimated numerically and verified experimentally. The motion responses are compared and discussed.

METHODOLOGY

A series of sea-keeping tests were performed to study the dynamic motion responses of truss spar model subjected to long and short-crested waves.

The wave tank and facilities

The experimental study was carried out at the Offshore Laboratory of Universiti Teknologi PETRONAS in the wave tank. The wave tank system comprises of wave-maker, remote control unit, signal generation computer and dynamic wave absorption beach. The wave tank measured 22 m long by 10 m wide by 1.5 m deep. The wave maker is capable of generating up to 0.45 m and period as short as 0.5 s (model scale). Major random sea spectra such as JONSWAP, ISSC, PM, Bretschneider, and Ochi-Hubble, can be simulated. Also, custom spectra can be added to the software and calibrated. Figs 1~2 show the wave tank in the Offshore Laboratory with 16 individual paddles for wave generation. Table 1 shows the details of the wave generator.

Table 1 Details of wave generator

Wave generator description	
Paddle width	0.62m
Paddles per module	8 Nos.
Module width	4.98m
No. module	2 Nos.
Maximum water depth	1.0m
Sea-states available	
• Regular Waves	
• Bi-directional Waves	
• Multi-directional Waves	
• WNSD (Random Waves with/without set down compensation)	
• Externally Generated Seas	

To record the motion responses of the model during the sea-keeping test, optical tracking system have been chosen. This system is defined as a method to obtain the position of an object by determining the active and passive positions through the marker reflections attached on the object by a camera capturing system. In the test series, the markers were placed on top of the model, and four cameras were used. Figs 3~4 show the components of the optical tracking system and the model setup with the optical tracking system. Other components that are integrated in the wave tank tests are the wave probes to record the wave profile, load cells to measure the mooring line tension, and accelerometers to record the acceleration of the model during the test.

Fig. 1 Wave tank of Offshore Laboratory

Fig. 2 Wave generator paddles

Fig. 3 Components of optical tracking system

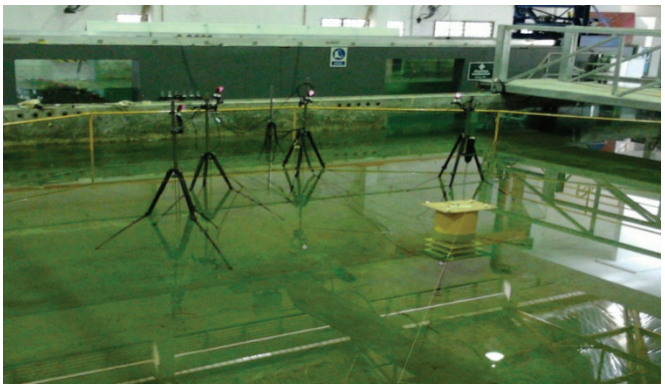

Fig. 4 Model setup with optical tracking system

Model description

A truss spar model with scale of 1:100 was fabricated using steel plates. The model was positioned in the tank and restrained by four linear springs connected to the steel wires at each quarter as mooring lines. The motion of the model was measured by the optical tracking system as discussed before. Table 2 shows the structural dimensions of the truss spar model and prototype. Figs. 5~7 show truss spar model configuration and the plan view of the experimental setup.

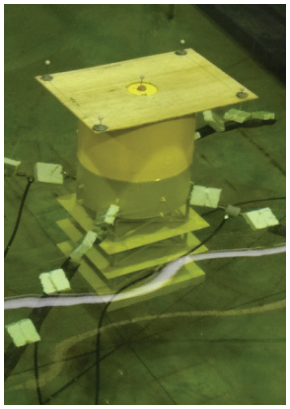

Fig. 5 Truss spar model

Details of wave

In this study, uni-directional regular wave and multi-directional wave by filtered white noise wave (WNSD) were generated. The multi-directional wave by filtered white noise wave considered the multi-directional waves as a product of wave spectrum and spreading function. In this study, the cosine square and Mitsuyasu spreading function incorporated in the JONSWAP wave spectrum were considered. In Table 3, the details of the uni and multi-directional waves generated are listed.

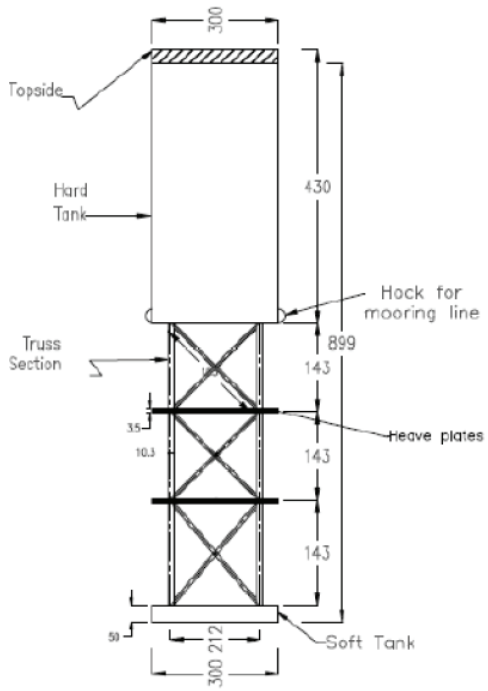

Fig. 6 Truss Spar Model Configurations (in mm)

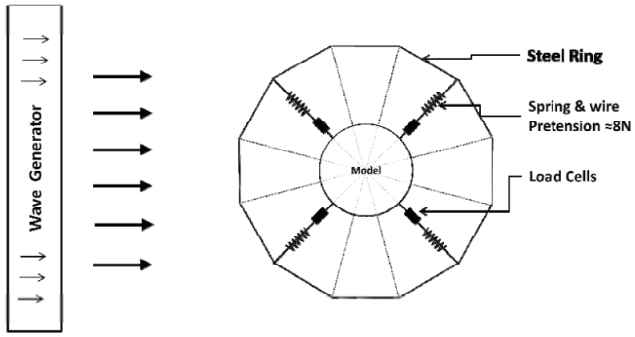

Fig. 7 Plan view of the experimental setup

Sea-keeping test

Multi-directional waves were generated in the sea-keeping test, to investigate the motion responses of the model in the real sea condition. Also, the uni-directional waves were generated to compare the responses by both waves to study the effectiveness of the short-crested wave statistics. In the test series, the fore and aft side of the model were restrained by soft spring and steel wires. Then, series of wave data discussed above were programmed and generated by the wave generator. In the test, motion response of the model in surge, heave and pitch were recorded by the optical tracking system.

Table 2 Structural dimensions of the truss spar model and prototype

Variable	Model	Prototype
Hull		
Diameter,m	0.300	12.00
Total Length,m	0.430	17.20
Draft,m	0.225	9.00
Wall Thickness,m	0.002	0.08
Truss section		
Diameter,m	0.01	0.40
Diagonal Length,m	0.256	10.24
Nos. Diagonal member	24	24
Vertical Length,m	0.143	5.72
Nos. Vertical member	12	12
Wall Thickness,m	0.002	0.08
Soft tank		
Nos. Vertical Plate	4	4
Length,m	0.300	12.00
Depth,m	0.050	2.00
Nos. Horizontal Plate	2	2
Length,m	0.300	12.00
Depth,m	0.300	12.00
Wall Thickness,m	0.002	0.08

Table 3 Wave series generated

Regular Wave		
Wave frequency, Hz	Wave Period, s	Wave Height, m
1.67	0.6	0.04
1.43	0.7	0.04
1.25	0.8	0.04
1.11	0.9	0.05
1.00	1.0	0.05
0.83	1.2	0.05
0.71	1.4	0.06
0.63	1.6	0.06
0.56	1.8	0.07
0.50	2.0	0.07
Multi-directional wave		
0.50	2.00	0.08
0.63	1.60	0.08
0.71	1.40	0.07
0.83	1.20	0.07
1.00	1.00	0.06
1.25	0.80	0.06

Post processing of data

The raw data obtained from the optical tracking system were analyzed and post processed by the Discrete Fast Fourier Transformation method to determine the response spectra. In this study, responses in term of response amplitude operator (RAO) were considered. The RAO was taken as:

$$RAO = \sqrt{\frac{S_R(f)}{S(f)}} \quad (1)$$

Where $S_R(f)$ is given as the motion response spectrum for the model , $S(f)$ is the wave spectrum and f is the wave frequency.

Numerical analysis

A MATLAB code was developed to study the motion responses of the truss spar by integrating the diffraction effects, which occur due to the large size of the hull. In this numerical simulation, the truss spar was modeled as a rigid body restrained by mooring lines with three degrees of freedom. The mass, damping and stiffness matrices were evaluated for every time step; and the equations of motion for the platform dynamic equilibrium were formulated and solved using Newmark beta method.

Zhu (1993) studied the diffraction of short crested wave around a circular cylinder, where the water run-up and the pressure distribution were taken around the cylinder. In this simulation, similar concept was considered that the surge diffraction force equation was obtained by integrating the total length of the spar cylindrical hull, and soft tank. The surge diffraction force for truss spar hull subjected to short crested waves was given as (Zhu, 1993)

$$F_{x\,hull} = \int_{-h}^{0} \frac{dFz}{dz} dz \quad (2)$$

$$F_{x\,hull} = \int_{-h}^{0} -2\pi\rho g r H \frac{\cosh k(z+d)}{\cosh kd} e^{-i\omega t} R(k_x,k_y,k,r) dz \quad (3)$$

Where

$$R(k_x,k_y,k,r) = i\left[R_0(k_x,k_y,k,r) + \sum_{n=1}^{\infty} R_n(k_x,k_y,k,r)\right] \quad (4)$$

$$R_0(k_x,k_y,k,r) = J_1(k_x r)J_0(k_y r) - \frac{k_x J_1'(k_x r)J_0(k_y r) + k_x J_1(k_x r)J_0'(k_y r)}{kH_1'(kr)} H_1(kr) \quad (5)$$

$$R_n(k_x,k_y,k,r) = i^{2n}\left\{\begin{matrix}\left[J_{2n+1}(k_x r)J_{2n}(k_y r) - B_{2n+1}H_1(kr)\right] - \\ \left[J_{2n-1}(k_x r)J_{2n}(k_y r) - B_{2n-1}H_1(kr)\right]\end{matrix}\right\} \quad (6)$$

The surge diffraction force for soft tank of the truss spar was given as

$$F_{x\,soft\,tank} = \int_{stb}^{stt} -2\pi\rho g r H \frac{\cosh k(z+d)}{\cosh kd} e^{-i\omega t} R(k_x,k_y,k,r) dz \quad (7)$$

In evaluating the heave force, double integration of the dynamic pressure on the bottom surface of the spar hull, b, which derived from Bernoulli equation and the potential velocity, was performed. The heave diffraction force was given as

$$F_x = \iint \left[\rho g r \frac{\cosh k(z+d)}{\cosh kd}\cos\theta + \frac{3}{4}\rho g \frac{\pi H^2}{L}\frac{1}{\sinh 2kd}\left(\frac{\cosh 2k(z+d)}{\sinh^2 kd} - \frac{1}{3}\right)\cos 2\theta - \frac{1}{4}\rho g \frac{\pi H^2}{L}\frac{1}{\sinh 2ks}(\cosh 2k(z+d) - 1\right] \partial b \quad (8)$$

Similar expression was considered to predict the heave force for heave plates and soft tanks, where b and z will be replaced by the respective surface elevations and vertical coordinates respectively.

The total moment about the axis parallel to the y-axis passing through the bottom of the cylinder was given as

$$M_{y\,hull} = \int_{-h}^{0} (z+d) F_{x\,hull} dz \quad (9)$$

$$M_{y\,soft\,tank} = \int_{stb}^{stt} (z+d) F_{x\,soft\,tank} dz \quad (10)$$

To solve the equations of motion, Newmark beta method was considered. The equation of motion was given as

$$F(t) = M\ddot{x} + Kx \quad (11)$$

[M] and [K] are taken as the mass and stiffness matrices; $\ddot{x}$ and x is defined as the structural acceleration and displacement. The total mass matrix, which defined in eq.(12) consisted of two components i.e. the structural mass matrix and added mass matrix. The total stiffness matrix defined in eq.(19) was considered as a summation of the hydrostatic and mooring stiffness matrix.

The total mass matrix [M] was given as

$$[M] = \begin{bmatrix} m & 0 & 0 \\ 0 & m & 0 \\ 0 & 0 & I \end{bmatrix} + \begin{bmatrix} m_{11} & m_{12} & m_{13} \\ m_{21} & m_{22} & m_{23} \\ m_{31} & m_{32} & m_{33} \end{bmatrix} \quad (12)$$

where *m* and *I* are the body mass and mass moment of inertia about y-axis. The structure was integrated from the bottom of the structure to the mean water level to predict the added mass, where the elements of added mass matrix are given as

$$m_{11} = \rho \frac{\pi D}{4} (C_M - 1) \cos^2 \Theta \, \partial z \quad (13)$$

$$m_{12} = m_{21} = -\rho \frac{\pi D}{4} (C_M - 1) \cos \Theta \sin \Theta \, \partial z \quad (14)$$

$$m_{13} = m_{31} = -\rho \frac{\pi D}{4} (C_M - 1) z \cos \Theta \, \partial z \quad (15)$$

$$m_{22} = \rho \frac{\pi D}{4} (C_M - 1) \sin^2 \Theta \, \partial z \quad (16)$$

$$m_{23} = m_{32} = \rho \frac{\pi D}{4} (C_M - 1) z \cos \Theta \, \partial z \quad (17)$$

$$m_{33} = \rho \frac{\pi D^2}{4} (C_M - 1) z^2 \, \partial z \quad (18)$$

where *z* is the distance of center of gravity to the keel of the hull with 1m increment for each element.

The stiffness matrix was given as

$$[K] = \begin{bmatrix} 0 & 0 & 0 \\ 0 & k_2 & 0 \\ 0 & 0 & k_3 \end{bmatrix} + \begin{bmatrix} k_x & 0 & k_x h_2 \\ 0 & 0 & 0 \\ k_x h_2 & 0 & k_x h_2^2 \end{bmatrix} \quad (19)$$

$$k_2 = \pi \rho g \left(\frac{D}{2}\right)^2 \quad (20)$$

Wherek_3 is defined as the buoyancy force by the distance from center of gravity to center of buoyancy, $h_2$distance from center of gravity and fairlead. k_x is the horizontal spring stiffness taken as a nonlinear function of the structure displacement that will be updated for each of the new displacement.

Newmark-Beta integration was adopted to solve the equations of motion, where in each time step the displacement of the structure was calculated, and was given as

$$\mathrm{X}_{t+\Delta} = \widehat{\mathrm{K}}^{-1} \widehat{\mathrm{F}}_{t+\Delta} \quad (21)$$

The effective stiffness matrix, $\hat{K}$ was given as

$$\widehat{\mathrm{K}} = \mathrm{K} + \mathrm{a}_0 \mathrm{M} \quad (22)$$

Then the acceleration,$\ddot{\mathrm{X}}_{t+\Delta t}$, and the velocity, $\dot{\mathrm{X}}_{t+\Delta t}$of the structure were calculated as

$$\ddot{\mathrm{X}}_{t+\Delta t} = \mathrm{a}_0 (\mathrm{X}_{t+\Delta} - \mathrm{X}_t) - \mathrm{a}_2 \dot{\mathrm{X}}_t - \mathrm{a}_3 \ddot{\mathrm{X}}_t \quad (23)$$

$$\dot{\mathrm{X}}_{t+\Delta t} = \dot{\mathrm{X}}_t + \mathrm{a}_6 \ddot{\mathrm{X}}_t + \mathrm{a}_7 \ddot{\mathrm{X}}_{t+\Delta t} \quad (24)$$

The effective loading matrix, $\widehat{\mathrm{F}}_{t+\Delta t}$ was formulated as

$$\widehat{\mathrm{F}}_{t+\Delta t} = \mathrm{F}_{t+\Delta t} + \mathrm{M}\left(\mathrm{a}_0 \mathrm{X}_t + \mathrm{a}_2 \dot{\mathrm{X}}_t + \mathrm{a}_3 \ddot{\mathrm{X}}_t\right) \quad (25)$$

The integration constants of Newmark-Beta method were taken as follow to solve the equation of motion.

$$\mathrm{a}_0 = 1/(\alpha \Delta \mathrm{t}^2) \quad (26)$$

$$\mathrm{a}_1 = \delta/(\alpha \Delta \mathrm{t}) \quad (27)$$

$$\mathrm{a}_2 = 1/(\alpha \Delta \mathrm{t}) \quad (28)$$

$$\mathrm{a}_3 = (1/2\alpha) - 1 \quad (29)$$

$$\mathrm{a}_4 = (\delta/\alpha) - 1 \quad (30)$$

$$\mathrm{a}_5 = (\Delta \mathrm{t}/2)[(\delta/\alpha) - 2] \quad (31)$$

$$\mathrm{a}_6 = \Delta \mathrm{t}(1 - \delta) \quad (32)$$

$$\mathrm{a}_7 = \delta \Delta \mathrm{t} \quad (33)$$

Where δ=0.5, α=0.25*(0.5+δ) 2, and Δt was take as time step.

RESULTS AND DISCUSSION

The dynamic motion responses of the truss spar subjected to the short crested waves were investigated in this study. In Figs 8 and 9, the wave profile for multi-directional short-crested waves and uni-directional regular long-crested waves are shown.

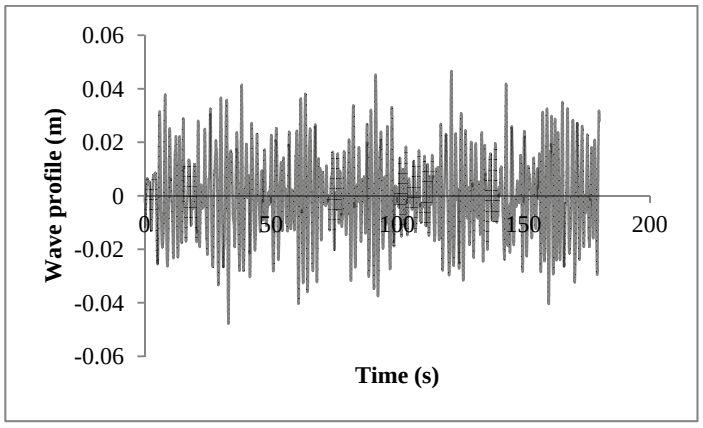

Fig. 8 Multi-directional wave profile

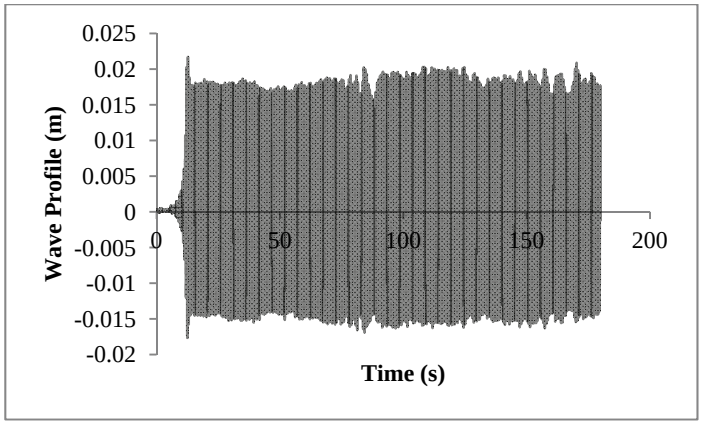

Fig. 9 Uni-directional regular wave profile

Figure 10 shows the measured surge responses and Figure 11 shows the comparison of the surge RAOs measured experimentally and predicted numerically. In Figure 11, it can be observed that the trend of the numerical and experimental surge RAOs agreed fairly well with the RAOs decreasing as the frequency increases. Above 0.07 Hz, the numerical RAOs were higher than the experimental RAOs.

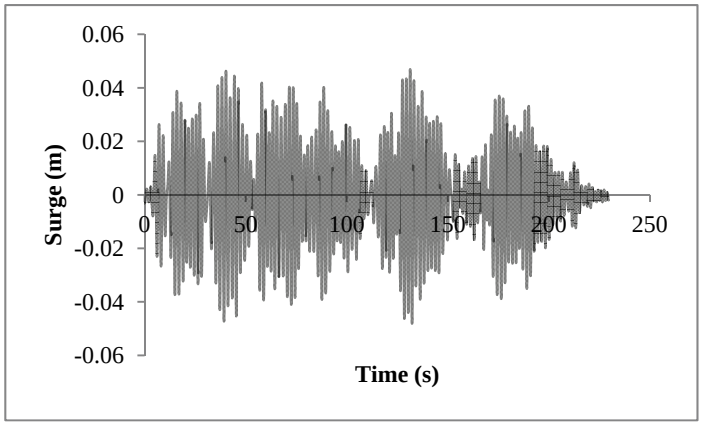

Fig. 10 Measured surge responses

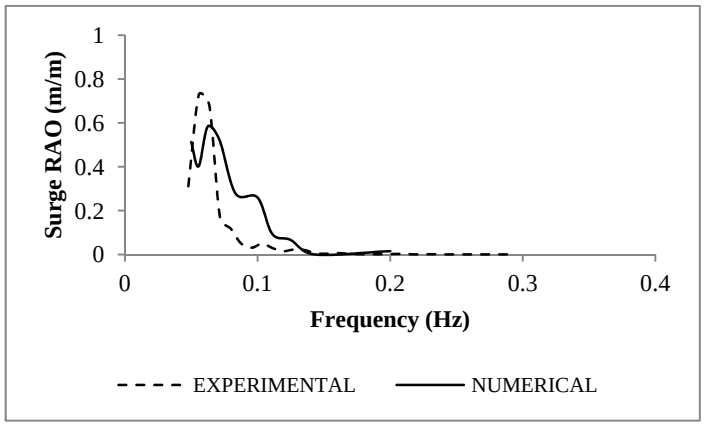

Fig.11 Experimental and numerical surge RAO

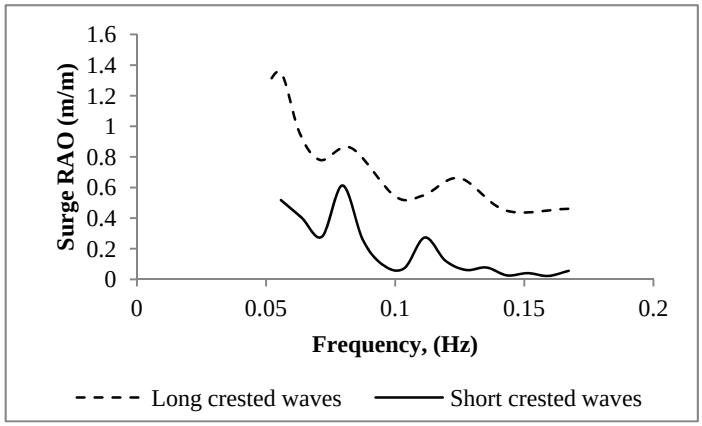

Fig. 12 Surge RAO due to long and short crested waves

In Figure 12, the surges RAOs due to long and short-crested waves are compared. It was found that the trends due to both waves are similar. However, significant variation could be observed in the magnitudes. The RAO due to long-crested waves yielded greater responses compared to the short-crested waves. The short-crested wave response was only about 10-40% of the long-crested wave response as the frequency decreased.

Figure 13 shows the heave motion responses measured for multi-directional waves and Figure 14 shows the comparison of the measured and predicted heave RAOs. In Figure 14, the trend and magnitude of the measured and predicted RAOs agreed well.

Figure 15 shows the comparison of heave RAO due to long and short-crested waves. For frequencies above 0.8Hz, the trend of both the long and short-crested waves agreed well. However, the magnitude of the RAOs due to long-crested was greater compared to the short-crested waves. At the low frequency region, the difference was much greater.

Figure 16 shows the time series for the measured pitch motion responses. Figure 17 shows the comparisons of predicted and measured RAOs. It could be observed that the trend of experimental measured RAOs agreed with the numerical pitch RAOs with maximum difference of about 30% at 0.075Hz. The experimental values were higher than the numerical values except for a small range of high frequency region above 0.175Hz. Figure 18 shows the pitch RAO

comparison due to the long and short-crested waves. It was found that generally the trends agreed fairly well. Also, it was found that the RAO subjected to the long-crested waves are almost double that of short-crested waves except for the frequency range 0.65 to 0.85 Hz.

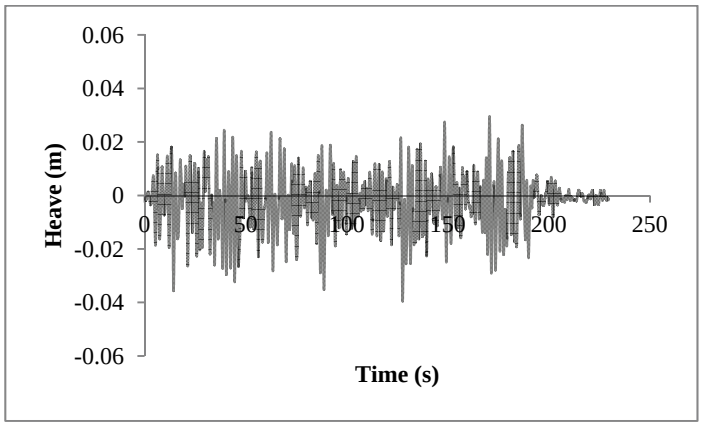

Fig. 13 Measured heave responses

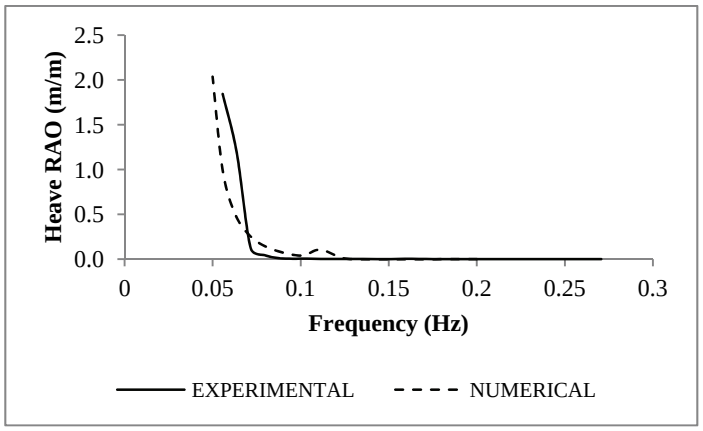

Fig. 14 Experimental and numerical heave RAO

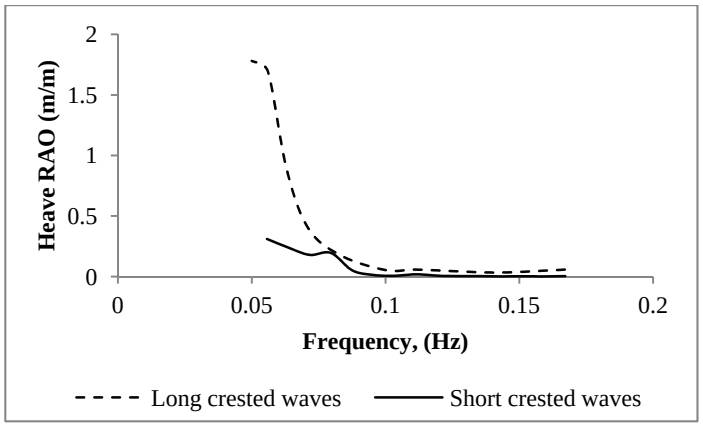

Fig. 15 Heave RAO due to long and short crested waves

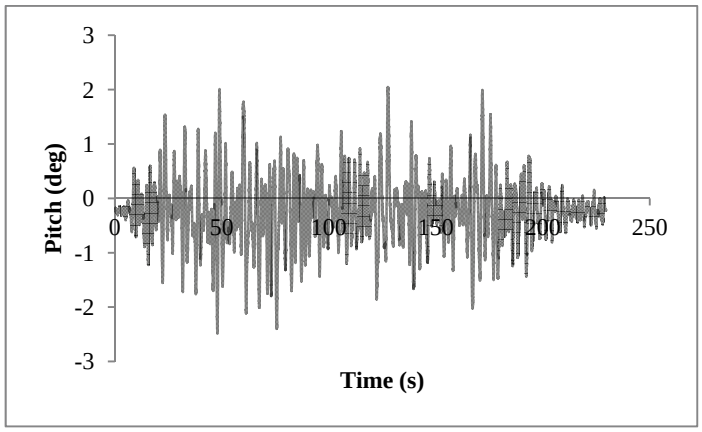

Fig. 16 Measured pitch responses

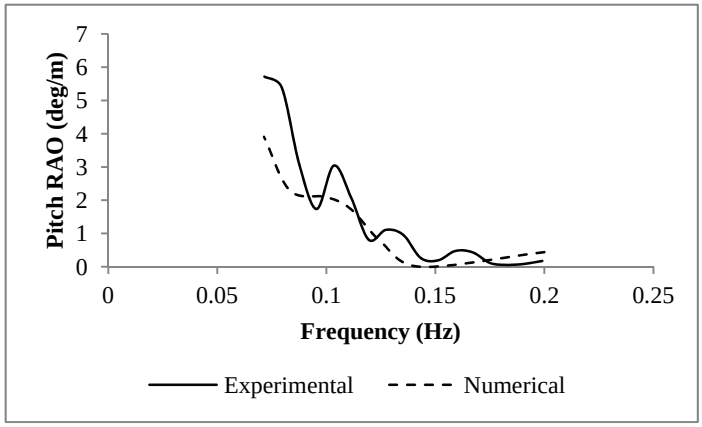

Fig. 17 Experimental and numerical pitch RAO

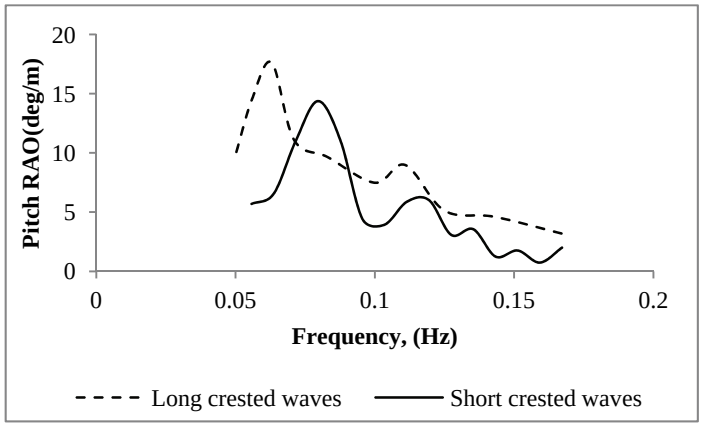

Fig. 18 Pitch RAO due to long and short crested waves

CONCLUSION

A series of experiments were performed to study the dynamic responses of the truss spar due to the short-crestedness of the waves. In the experiments, a 1:100 scaled truss spar model restrained with linear spring and steel wires was tested. The short-crested wave responses from the numerical are compared with the experimental measured

responses for validation. From the comparison, it was found that the results agreed fairly well in the trend. The effectiveness of the short-crested wave statistics was studied by comparing the responses due to long and short-crested waves. It was observed that the short-crested waves yielded smaller responses compared to the long-crested waves. Hence, it could be confirmed that by adopting the short-crested wave statistics, a more economical design would be arrived at.

From the study, the following conclusions were drawn:

1. The numerical time domain simulation was able to predict the dynamic responses fairly well. The trends agreed for the surge, heave and pitch responses. The numerical values for surge and pitch responses were lower compared to the experimental values and the numerical values for heave responses were higher.
2. The responses due to short-crested waves for surge, heave and pitch were much lower compared to the responses for long-crested waves. Further studies on this can confirm the same. If this fact is very well established, it can lead to much more economical design of offshore platforms based on the availability of multi-directional wave statistics.

REFERENCES

Aage, C., (1990). "Applicability of 3D wave loads in offshore design", *Environmental Forces on Offshore Structures and Their Predictions*, Vol. 26, pp 247-260.

Borgman, L. E., (1969). "Directional spectra models for design use", *Offshore Technology Conference*, pp 721 – 736.

Chakrabarti S.K., (2001), *Hydrodynamic of Offshore Structures*, WIT Press, 420 pp.

Fernandes A.A., Sarma Y.V.B, and Menon H.B., (2000)."Directional spectrum of ocean waves from array measurements using phase/time/path difference methods", *Ocean Engineering*, Vol 27, pp 345 – 363.

Haver S., (1990) "On the modeling of short crested sea for structural response calculations", *Proc of the First (1990) European Offshore Mechanics Symposium*, Trondheim, Norway, ISOPE, 20-22 August 1990.

Hisaki Y., (2006) "Ocean wave directional spectra estimation from an HF ocean radar with a single antenna array: Methodology", *Journal of Atmospheric and Ocean Technology*, Vol. 23, pp 268 – 286.

Hogben N. and Cobb F.C., (1986) "Parametric modeling of directional wave spectra", *Offshore Technology Conference*, pp 1 – 10.

Huntington S. M. and Thompson D.M., (1976) "Forces on a large vertical cylinder in multi-directional random waves", *Offshore Technology Conference*, pp 169 – 175.

Huntington S.W. and Gilbert G.,(1979). "Extreme forces in short crested seas", *Offshore Technology Conference*, pp 2075-2081, 1979.

Jian Y.J., Zhan J.M., Zhu Q.Y., (2008), "Short crested wave-current forces around a large vertical circular cylinder", *European Journal of Mechanics B/Fluids*, Vol 27, pp 346-360.

Kumar V.S., Deo M.C., Ananda N.M. and Chandramohan P., (1999) "Estimation of wave directional spreading in shallow water", *Ocean Engineering*, Vol. 26, pp 83 – 98.

Kumar V.S., Deo M.C., Anand N.M., and Kumar K.A., (2000) "Directional spread parameter at intermediate water depth", *Ocean Engineering*, Vol. 27, pp 889-905.

Kumar V.S. and Anand N.M., (2004)."Variations in wave direction estimated using first and second order Fourier coefficients", *Ocean Engineering*, Vol. 31, pp 2105 – 2119.

Kurian V.J., Ng C.Y. and Liew M.S., "Dynamic Responses of Truss Spar Due to Wave Actions,",*Research Journal of Applied Sciences, Engineering and Technology*

Li D., (1980) "Encounter spectra and digital simulations of short crested sea waves", PhD dissertation, Columbia University.

Moon, I.J., Gints I., Hara T., Tolman H.L. Wright C.W. and Walsh E.J., (2003). "Numerical simulation of sea surface directional wave spectra under hurricane wind forcing", *Journal of Physical Oceanography*, Vol. 33, pp 1680-1706.

Zhu S., (1993). "Diffraction of short crested waves around a circular cylinder", *Ocean Engineering*, Vol. 20. No. 4, pp 389-407.

Zhu S. and Moule G., (1994)."Numerical calculation of forces induced by short crested waves on a vertical cylinder with arbitrary cross section", *Ocean Engineering*, Vol. 21, No.7, pp 645-662.

Zhu S., SatravahaP.,(1995). "Second-order wave diffraction forces on a vertical circular cylinder due to short crested waves", *Ocean Engineering*, Vol. 22, No. 2, pp 135-189.